Solution of a quantum mechanical eigenvalue problem with long range potentials

Frank H. Stillinger
Bell Telephone Laboratories, Murray Hill, New Jersey, 07974

(Received 13 February 1979; accepted for publication 27 April 1979)

Wavefunctions and eigenvalues for the Schrödinger equation on the half-line $x \geq 0$ are examined in the presence of a potential $v_0 x^{-2} + v_1 x^{-1} + v_2 x^{-1/2}$. With a special choice for the constant v_0 the wave equation can be solved in terms of parabolic cylinder functions. In this case the spectrum is determined by an implicit equation that arises from the boundary condition that must be imposed at $x = 0$. Depending on v_1 and v_2, the spectrum can contain and infinite number of discrete values, a finite number, or none. It is pointed out that continuous variations in v_1 or v_2 can convert negative energy bound states into positive energy responances, or *vice versa*, and the threshold behavior has been investigated.

I. INTRODUCTION

It is often enlightening to achieve exact solutions to model problems in quantum mechanics, even though the models may not directly represent physically realizable systems. The example treated in this paper largely fits that description. It entails the exact determination of wavefunctions and energy levels for a single particle subject to a central potential of the form

$$V(r) = v_0 r^{-2} + v_1 r^{-1} + v_2 r^{-1/2}. \tag{1.1}$$

The method of solution requires that v_0 have a definite value; however v_1 and v_2 are arbitrary, and the resulting flexibility in V generates an interesting richness of behavior.

The following Sec. II provides some preliminary transformations which facilitate the solution of selected quantum-mechanical problems in terms of parabolic cylinder functions. Section III shows how the spectrum specifically for potential (1.1) must be determined in principle, while Sec. IV carries that determination to essential completion. Continuum solutions are examined in Sec. V.

One of the primary reasons for interest in the model potential (1.1) is that it can produce sharp resonance behavior. If $v_1 < 0$ and $v_2 > 0$, $V(r)$ will display a wide barrier around an attractive core region. Presuming that v_1 is sufficiently negative to produce bound states, variation in v_2 can move their energies up or down, and in particular can move a bound state to zero energy (the continuum edge). This special circumstance which separates bound-state character from resonance character is studied to some extent here with emphasis on threshold behavior (Secs. IV and V). However, we intend the present work to serve as the foundation for a later, more complete analysis of these continuum edge encounters.

II. PRELIMINARY TRANSFORMATIONS

Our objective is construction of a class of solutions over $x \geqslant 0$ for the one-dimensional Schrödinger equation

$$\Phi''(x) + B(x)\Phi(x) = 0 \tag{2.1}$$

subject to suitable boundary conditions. Upon introduction of appropriate reduced units one has

$$B(x) = 2E - 2V(x), \tag{2.2}$$

where E is the total energy and $V(x)$ is the potential energy function. Equation (2.1) is also relevant to the radial motion with a central potential $V(r)$ in a space of D dimensions.[1] For that case the radial wavefunction $R(r)$ may be written

$$R(r) = r^{(1-D)/2}\Phi(r), \tag{2.3}$$

where Φ is a solution to Eq. (2.1) with

$$B(x) = 2E - 2V(x) - C(D, \Lambda)x^{-2}, \tag{2.4}$$

and

$$C(D, \Lambda) = \Lambda(\Lambda + D - 2) + \tfrac{1}{4}(D-1)(D-3). \tag{2.5}$$

In this last expression $\Lambda = 0,1,2,\cdots$ is the quantum number for angular momentum.

If Φ can be expressed in the form

$$\Phi(x) = f(x)\phi[g(x)], \tag{2.6}$$

then direct substitution shows that the differential equation (2.1) will be satisfied provided ϕ is a solution to

$$\phi'' + \left[\frac{2f'}{fg'} + \frac{g''}{(g')^2}\right]\phi' + \left[\frac{f''}{f(g')^2} + \frac{B}{(g')^2}\right]\phi = 0. \tag{2.7}$$

It will be advantageous to eliminate the ϕ' term. This will occur by requiring f to be determined by g in the manner:

$$f = C_0(g')^{-1/2}, \tag{2.8}$$

where C_0 is any nonzero constant. Thereupon the differential equation for ϕ adopts the following form:

$$\phi''(g) + \left[\frac{B}{(g')^2} - \frac{g'''}{2(g')^3} + \frac{3(g'')^2}{4(g')^4}\right]\phi(g) = 0. \tag{2.9}$$

We will now demand that the coefficient of ϕ in Eq. (2.9) be quadratic in g,

$$\phi''(g) + (ag^2 + bg + c)\phi(g) = 0, \tag{2.10}$$

where a, b, and c are constants. In other words, we demand that ϕ obey the general differential equation for parabolic cylinder functions.[2] Therefore, we will have

$$B(x) = \frac{g'''}{2g'} - \frac{3(g'')^2}{4(g')^2} + (g')^2(ag^2 + bg + c). \tag{2.11}$$

 0022-2488/79/091891-05$01.00

Next it is necessary to identify functions $g(x)$ which upon substitution in Eq. (2.11) will confer upon $B(x)$ the requisite form (2.4) or (2.2). In doing so we must ensure that the x independent term in $B(x)$ can sweep through all possible values for $2E$ to avoid missing any eigenvalues. Several simple examples can be listed.

(1) By choosing

$$g(x) = x, \tag{2.12}$$

one obtains

$$B(x) = ax^2 + bx + c. \tag{2.13}$$

This is the form appropriate for the one-dimensional harmonic oscillator with

$$V(x) = -\frac{a}{2}\left(x + \frac{b}{2a}\right)^2, \qquad E = \frac{c}{2} - \frac{b^2}{8a}, \tag{2.14}$$

provided $a < 0$. After selecting a and b to represent appropriately the curvature and position of the quadratic potential, independent variation of c will yield any E value, including the well-known spectrum of equally spaced eigenvalues.

(2) With the choice

$$g(x) = x^{2/3}, \tag{2.15}$$

Eq. (2.11) yields

$$B(x) = (5/36x^2) + (4/9)(ax^{2/3} + b + cx^{-2/3}). \tag{2.16}$$

It is known on general grounds[3] that an x^{-2} term in $B(x)$ would prevent occurrence of any eigenstates provided its coefficient exceeded 1/4. However, that does not happen here. One could therefore proceed to determine energies and eigenfunctions for the case ($a \leqslant 0$):

$$V(x) = -\frac{5}{72x^2} - \frac{2ax^{2/3}}{9} - \frac{2c}{9x^{2/3}}, \qquad E = \frac{2b}{9}. \tag{2.17}$$

(3) The case of primary interest in this paper corresponds to

$$g(x) = x^{1/2}, \tag{2.18}$$

for which

$$B(x) = (3/16x^2) + (1/4)(a + b/x^{1/2} + c/x). \tag{2.19}$$

Once again an inverse square term arises with a magnitude consistent with the existence of eigenstates. The natural separation of B is obviously the following:

$$V(x) = -\frac{3}{32x^2} - \frac{b}{8x^{1/2}} - \frac{c}{8x}, \qquad E = \frac{a}{8}. \tag{2.20}$$

We shall see in detail how the signs and magnitudes of b and c determine whether the number of eigenstates is infinite, finite and positive, or zero.

III. SPECTRUM DETERMINATION

Case 3 above leads to the following generic wavefunction:

$$\Phi(x) = 2^{1/2}C_0 x^{1/4}\phi(x^{1/2}), \tag{3.1}$$

where ϕ is a solution to Eq. (2.10) over the positive real axis. In this section we shall be concerned with bound states, i.e., $a < 0$. Setting

$$g = \frac{z}{2^{1/2}|a|^{1/4}} + \frac{b}{2|a|}, \qquad \phi(g) = w(z), \tag{3.2}$$

Eq. (2.10) transforms to one of the standard forms for parabolic cylinder functions[2]

$$w''(z) - (\tfrac{1}{4}z^2 + A)w(z) = 0, \tag{3.3}$$

where

$$A = -\frac{b^2}{8|a|^{3/2}} - \frac{c}{2|a|^{1/2}}. \tag{3.4}$$

The independent solutions to differential Eq. (3.3) are conventionally denoted by $U(A,z)$ and $V(A,z)$. The latter diverges as z approaches infinity; only the former is an acceptable solution. Thus,

$$\Phi(x) = 2^{1/2}C_0 x^{1/4}U\left(A, 2^{1/2}|a|^{1/4}x^{1/2} - \frac{b}{2^{1/2}|a|^{3/4}}\right) \tag{3.5}$$

encompasses all eignefunctions.

It is unacceptable on general grounds for $\Phi(x)$ to behave as $x^{1/4}$ at the origin; instead the leading order must be $x^{3/4}$ at this point.[3] Consequently $x = 0$ must be a zero of U in Eq. (3.5):

$$U\left(-\frac{b^2}{8|a|^{3/2}} - \frac{c}{2|a|^{1/2}}, -\frac{b}{2^{1/2}|a|^{3/4}}\right) = 0. \tag{3.6}$$

This condition will only be satisfied for a discrete set of negative a values which, through the second of Eqs. (2.20), determines the energy spectrum.

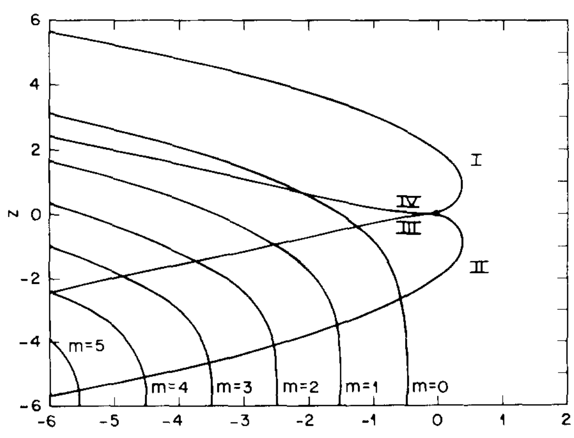

FIG. 1. Graphical determination of eigenvalues according to implicit Eq. (3.6). The curves labeled $m = 0,1,2,\cdots$ are loci of zeros for $U(A,z)$. The four curves emanating from the origin represent special cases of Eq. (4.1): I: $b = -1, c = -1$; II: $b = 1, c = -1$; III: $b = 1, c = 4$; IV: $b = -1$, $c = 4$.

IV. EIGENVALUE RESULTS

The task of deducing eigenvalues and their behavior is simplified considerably by using a graphical analysis in the real A, z plane. The roots of $U(A,z)$ correspond to curves in that plane, and their intersections with another curve determined by the form of Eq. (3.6) yield the energy spectrum. This last curve can be constructed by eliminating $|a|$ between the specific forms shown in Eq. (3.6) for the variables A and z, with the result

$$A = -\frac{z^2}{4} - \frac{c|z|^{2/3}}{2^{2/3}|b|^{2/3}}; \tag{4.1}$$

since

$$z = -\frac{b}{2^{1/2}|a|^{3/4}} \tag{4.2}$$

along this curve the sign of z is opposite to that of b.

Figure 1 shows the A, z plane with loci of zeros for $U(A,z)$, and selected examples of the curve (4.1) for each of the four sign assignments for b and c.

The following properties should be noted for the zeros of $U(A,z)$.

(1) The zeros occur along an infinite set of curves confined to the left half plane.

(2) Each curve intersects the negative A axis once and only once at a point of the form $-(2m+3/2)$, $m=0,1,2,\cdots$. The integer m is a convenient index for the curves.

(3) All of the curves lie below the upper branch of the parabola $A=-z^2/4$.

(4) For each curve $A(z)$ is a single-valued function with unique inverse and the property

$$\lim_{z\to-\infty} A(z) = -(m+1/2). \tag{4.3}$$

We now discuss each of the four sign assignments separately.

(i) $b<0$, $c<0$. By referring to Eq. (2.20) we see that this case makes both the $x^{-1/2}$ and the x^{-1} parts of the interaction repulsive. Since the attractive x^{-2} term alone is incapable of producing bound states[3] it is obvious that addition of these extra repulsions will not change that situation. The graphical manifestation is clear in Fig. 1, for curve (4.1) lies above the upper branch of the parabola $A=-z^2/4$ and hence cannot intersect any zeros of U.

(ii) $b>0$, $c<0$. The $x^{-1/2}$ term in $V(x)$ is now negative, but the x^{-1} term remains positive. Since the former will dominate V at large x and since it has such extreme range, it is clear that an infinite number of bound states should exist. This is also clear from Fig. 1, since the corresponding position of the curve for Eq. (4.1) lies below the lower branch of $A=-z^2/4$ and intersects each U-zero branch in turn. If the magnitude of the negative quantity c is very large, Eq. (4.3) may be used to derive the following limiting distribution of eigenvalues:

$$E \simeq -\frac{b^2}{32|c|} + \frac{b^3(m+1/2)}{32|c|^{5/2}}. \tag{4.4}$$

Such equally spaced levels are characteristic of harmonic oscillators, and indeed that is what this limit has generated. The interplay between attractive $x^{-1/2}$ and strongly repulsive x^{-1} potential terms gives $V(x)$ a negative broad minimum at

$$x_{\min} \simeq 4c^2/b^2, \tag{4.5}$$

in the neighborhood of which quadratic behavior obtains. The low-lying states in this case are sufficiently localized around $x_{\min}$ to resemble harmonic oscillator states, and Eq. (4.4) reflects that fact.

(iii) $b>0$, $c>0$. The potential is negative everywhere and of course long-ranged. The bound states are infinite in number, since curve (4.1) must cross each U-zero curve (see Fig. 1). As b shrinks to zero, the curve for Eq. (4.1) approaches the negative A axis. In this limit $V(x)$ contains no $x^{-1/2}$ part. Remark 2 above is relevant for locating intersections, and one obtains the Rydberg series

$$E(b=0) = -\frac{c^2}{128(m+3/4)^2}. \tag{4.6}$$

For small b it should be a relatively straightforward matter to calculate successive orders of perturbation to this last result.

(iv) $b<0$, $c>0$. This is the most interesting of the four cases in that the number of bound states depends crucially upon the magnitudes of b and c. It is also the case which permits resonances to exist since $V(x)$ will have a positive barrier.

As b changes continuously from positive to negative, the preceding case (iii) transforms to the present case with Rydberg series (4.6) marking the boundary between the two. Any given eigenvalue increases continuously as b decreases, since V is being made less attractive. As we shall now see, it is possible to decrease b to a point at which any given eigenvalue increases to zero and ceases to belong to the bound-state spectrum. This last phenomenon is associated with intersections in the second quadrant of Fig. 1 that recede to infinity. In order to identify conditions that produce such behavior, it suffices to have an asymptotic expansion, valid for large $|A|$, for the U-zero curve with index m in Fig. 1[4]:

$$z_m \sim 2|A|^{1/2} - \frac{(-a_{m+1})}{|A|^{1/6}} - \frac{(-a_{m+1})^2}{20|A|^{5/6}} + O(|A|^{-3/2}),$$
$$m=0,1,2,\cdots, \tag{4.7}$$

where a_n is the nth (negative) zero of the Airy function $\mathrm{Ai}(t)$. The first few a_n have the following values[5]:

$$\begin{aligned} a_1 &= -2.3381\ 0741,\\ a_2 &= -4.0879\ 4944,\\ a_3 &= -5.5205\ 5983,\\ a_4 &= -6.7867\ 0809. \end{aligned} \tag{4.8}$$

Equation (4.1) can be used for the intersections of interest to eliminate A from Eq. (4.7), and then z can be expressed in terms of a and b according to Eq. (3.6). Taking into account the second of Eqs. (2.20) we find (for $\Delta_m>0$),

$$E_m = -[15|b|^{4/3}/64(-a_{m+1})^2]\Delta_m + O(\Delta_m^2), \tag{4.9}$$

where

$$\Delta_m = a_{m+1} + c/|b|^{2/3}. \tag{4.10}$$

This shows that the mth eigenvalue vanishes when Δ_m vanishes, i.e., when

$$c/|b|^{2/3} = -a_{m+1}. \qquad (4.11)$$

For slightly larger values of $c/|b|^{2/3}$, E_m varies linearly with Δ_m. A more detailed analysis shows that higher order corrections in Eq. (4.9) involve only positive integer powers of the quantity Δ_m. It is easy to show that at threshold each bound state exhibits the following asymptotic exponential order:

$$\Phi(x) = \exp[-(2/3)|b|^{1/2}x^{3/4} + o(x^{3/4})]. \qquad (4.12)$$

Consequently the bound-state property of square integrability is retained at threshold.

V. CONTINUUM SOLUTIONS

All positive energy states are unbound, and they form a dense continuum. The second of Eqs. (2.20) establishes that $a > 0$ for these unbound states. In place of Eq. (3.2) for bound states, we now set

$$g = \frac{z}{2^{1/2}a^{1/4}} - \frac{b}{2a},$$
$$\phi(g) = w(z). \qquad (5.1)$$

Consequently w must satisfy

$$w''(z) + (\tfrac{1}{4}z^2 - A)w(z) = 0, \qquad (5.2)$$

$$A = \frac{b^2}{8a^{3/2}} - \frac{c}{2a^{1/2}}. \qquad (5.3)$$

The real solutions to parabolic cylinder Eq. (5.2) conventionally[2] are denoted by $W(A,z)$ and $W(A,-z)$. Consequently, aside from a normalization factor the general solution has the form

$$w(z) = \cos\theta W(A,z) + \sin\theta W(A,-z), \qquad (5.4)$$

where θ must be chosen to satisfy boundary conditions.

Just as was the case with bound states, continuum wavefunctions $\Phi(x)$ must behave as $x^{3/4}$ near the origin.[3] This in turn requires that $w(z)$ vanish when $x = 0$, that is when

$$z = \frac{b}{2^{1/2}a^{3/4}}. \qquad (5.5)$$

In order for this to occur θ must obey the following relation:

$$\tan\theta(a) = -\frac{W((b^2/8a^{3/2}) - (c/2a^{1/2}),(b/2^{1/2}a^{3/4}))}{W((b^2/8a^{3/2}) - (c/2a^{1/2}), -(b/2^{1/2}a^{3/4}))}. \qquad (5.6)$$

This completes the determination of positive energy states, at least in principle.

These continuum solutions are useful in locating resonances, i.e., complex energy states with pure diverging current boundary conditions at $x = +\infty$:

$$\ln\Phi_r \sim i(2E)^{1/2}x. \qquad (5.7)$$

Here E will have a negative imaginary part whose magnitude determines the resonance width in the usual way. Along with such a resonance there will also exist a time-reversed "antiresonance" state with pure converging-current boundary conditions:

$$\ln\Phi_{ar} \sim -i(2E^*)^{1/2}x. \qquad (5.8)$$

By using the large z asymptotic forms[2] for $W(A,z)$ and $W(A,-z)$ one can show that the resonance condition (5.7) leads to the following implicit equation:

$$U\left[i\left(\frac{b^2}{8a^{3/2}} - \frac{c}{2a^{1/2}}\right), \frac{b\exp(-\pi i/4)}{2^{1/2}a^{3/4}}\right] = 0. \qquad (5.9)$$

The complex resonance energies are again given by the second of Eqs. (2.20) now in terms of complex a values which satisfy Eq. (5.9). The analog of the last equation for the time-reversed states is

$$U\left[-i\left(\frac{b^2}{8a^{3/2}} - \frac{c}{2a^{1/2}}\right), \frac{b\exp(\pi i/4)}{2^{1/2}a^{3/4}}\right] = 0. \qquad (5.10)$$

For any solution a of Eq. (5.9), a^* solves (5.10).

Analytic connections can be established between bound states just below threshold and the corresponding resonance and antiresonance energy pair above threshold. This is accomplished by giving the originally real parameter b an infinitesimal imaginary part as it passes a threshold value. If the imaginary part is negative, Eq. (3.6) for bound states converts automatically to Eq. (5.9) for resonances. If the imaginary part is positive, Eq. (3.6) converts to Eq. (5.10) for antiresonances. Therefore, the bound state energy in the complex b plane displays a cut at threshold, with the resonance and antiresonance pair at corresponding positions along the cut.

It is significant that Eqs. (5.9) and (5.10) lead to *identically* the same small Δ_m series that was indicated in Eq. (4.9) for bound states at threshold, but now with negative Δ_m. This series, which is evidently asymptotic rather than convergent, yields a real result above threshold whereas we know that the resonance state has an imaginary part. Clearly this imaginary part has a zero asymptotic series in positive powers of Δ_m.

VI. DISCUSSION

Although it is proper to regard the potential $V(r)$ in Eq. (1.1) as artificial, it is worth noting that an electrostatic charge density $\rho(r)$ exists which would cause a unit charge to experience just that potential. By employing Poisson's equation, one finds the appropriate density in three dimensions to be

$$\rho(r) = v_0 \lim_{\epsilon\to 0} f(\epsilon,r) + v_1\delta(r) + v_2/16\pi r^{5/2}, \qquad (6.1)$$

where

$$f(\epsilon,r) = 3/2\pi\epsilon^4, \quad (0 \leqslant r < \epsilon),$$
$$= -1/2\pi r^4, \quad (\epsilon \leqslant r). \qquad (6.2)$$

Similar results can easily be obtained for other values of D, the space dimension.

There may be some interest eventually in comparing exact eigenvalues for the present model with those approximate semiclassical eigenvalues that follow from quantization of the classical action.[6-8] In this regard, we mention in passing that the general radial potential containing terms of arbitrary strength proportional to r^{-2}, $r^{-3/2}$, r^{-1}, and $r^{-1/2}$ is a case for which the classical equations of motion can be integrated in closed form using Legendre elliptic integrals of the first and third kinds.[9] The present model is just a special case of this more general potential.

The available theory of the asymptotic properties of parabolic cylinder functions[2,4] is not sufficient to provide the imaginary part of our resonance energies near threshold, as discussed in Sec. V above. In principle the necessary information could be achieved through direct numerical study of Eq. (5.9), though this is likely to be a cumbersome procedure. On this account it is useful to turn to the quasiclassical WKB method. That approximation indicates that the inverse lifetime just above threshold will be dominated by a factor of the type ($K > 0$),

$$\exp(-K/|\Delta_m|^{3/2}). \tag{6.3}$$

The imaginary part of the resonance energy is proportional to the inverse lifetime, and thus exhibits the same factor. Since (6.3) has a zero asymptotic series in positive powers of Δ_m we see that the WKB approximation is consistent with the failure of imaginary terms to appear in Eq. (4.9) for $\Delta_m < 0$.

The present model may provide a convenient testing ground for the method of complex coordinate rotation[10,11] that seems to be computationally useful for locating resonances.[12,13] In particular, the one-dimensional nature of our model should permit extensive studies to be carried out on the effect of various basis set choices in complex-coordinate-rotation calculations. The extent of agreement between the computed thresholds and the behavior of the real part of the energy there, in comparison with the exact result in Eq. (4.9), provides a natural measure of numerical accuracy. At the same time it would be instructive to see how resonance lifetimes predicted by such calculations compare with the WKB result.

The WKB approximation predicts that the energy in the complex b plane possesses an essential singularity at threshold. A natural sequel to the present study would therefore involve generating the first few terms in an exact b power series for eigenvalues. Standard methods of power series analysis could then be employed to test for a singularity of the WKB type at the known thresholds.

[1]F.H., Stillinger, J. Math. Phys. **18**, 1224 (1977).
[2]M. Abramowitz and I.A. Stegun, *Handbook of Mathematical Functions*, NBS Applied Mathematics Series, No. 55 (U.S. Government Printing Office, Washington, D.C., 1968), Chapter 19.
[3]L.D. Landau and E.M. Lifshitz, *Quantum Mechanics*, translated by J.B. Sykes and J.S. Bell (Addison–Wesley, Reading, Massachussetts, 1958), pp. 118–21.
[4]F.W.J. Olver, J. Res. Nat. Bur. Stand B **63**, 131 (1959).
[5]Ref. 2, p. 478.
[6]A. Einstein, Verhandl. deut. physik. Ges. **19**, 82 (1917).
[7]M.L. Brillouin, J. Phys. Paris **7**, 353 (1926).
[8]J.B. Keller, Ann. Phys. (N.Y.) **4**, 180 (1958).
[9]E.T. Whittaker and G.N. Watson, *A Course of Modern Analysis* (Cambridge U.P., 1952), p. 515.
[10]E. Balslev and J.M. Combes, Commun. Math. Phys. **22**, 280 (1971).
[11]B. Simon, Commun. Math. Phys. **27**, 1 (1972).
[12]T.N. Rescigno and W.P. Reinhardt, Phys. Rev. A **10**, 2240 (1974).
[13]G. Doolen, J. Nuttall, and R. Stagat, Phys. Rev. A **10**, 1612 (1974).